Qeios

Why Mature Galaxies Seem to Have Filled the Universe Shortly After the Big Bang — A New Cosmological Model, that Predicted the JWST Observations

Arthur Pletcher

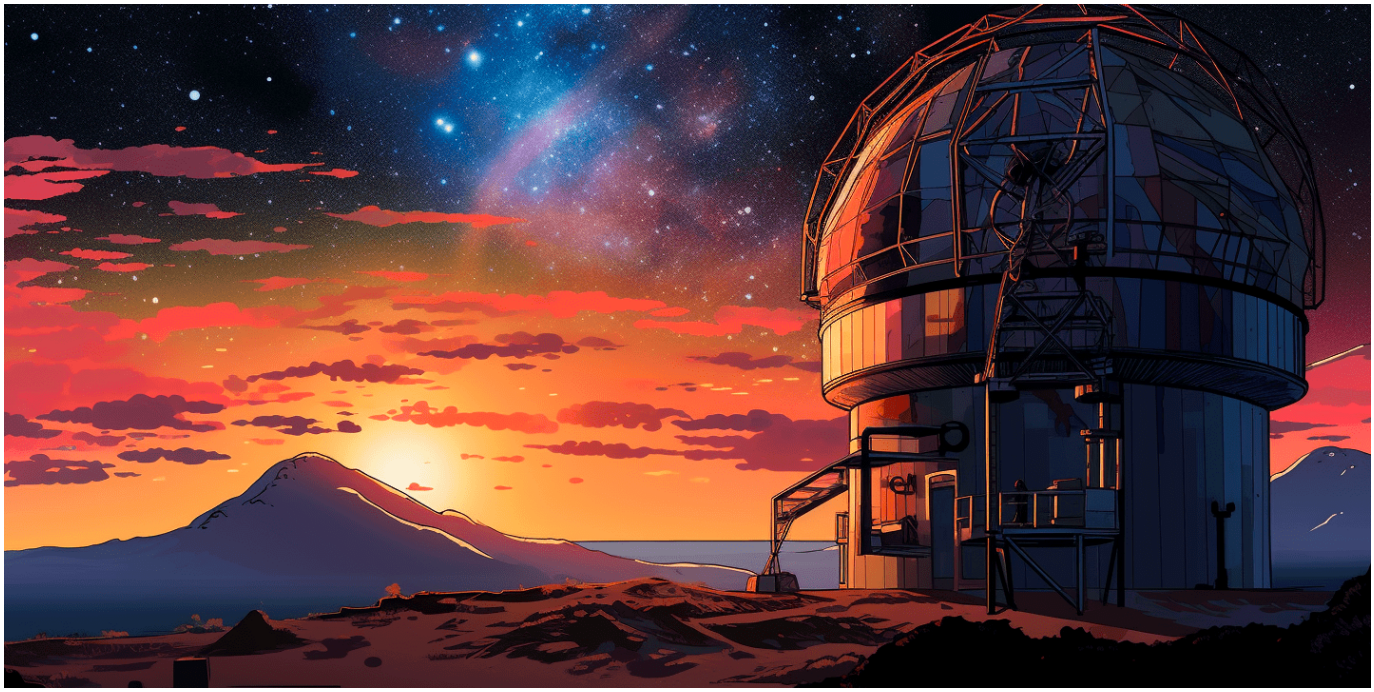

v4

Jan 19, 2024

https://doi.org/10.32388/2X1GDL.4

Why Mature Galaxies Seem to have Filled the Universe shortly after the Big Bang
A New Cosmological Model, that Predicted the JWST Observations

January 19, 2024

Arthur E. Pletcher [1]
[1] *International Society for Philosophical Enquiry, Woodbridge, VA, USA*
artpletcher@ultrahighiq.org

Abstract

Recent observations from the first dataset, provided by NASA's James Webb Space Telescope (JWST) of six massive galaxies, at a time in the early universe, seem to defy conventional cosmological models, as they appear to be as mature and developed as our own local group. Such unexpected discoveries **justify a radically novel model of Cosmology. To quote Joel Leja, assistant professor of astronomy and astrophysics at Penn State "It turns out we found something so unexpected it actually creates problems for science. It calls the whole picture of early galaxy formation into question"**. This article provides an alternative mathematical model of cosmological redshifting (z), which actually predicted such mature galaxies in a 2022 preprint, prior to these recent observations. As well, this model also predicts discrepancies between theoretical and observed galaxy rotation curves with apparent increased energy density.
The Azimuthal Projection Model of Universe is conceptualized as an $\mathbb{R}^5$ spacetime, with a four spatial dimensional hyperspere azimuthally projected onto a three spacial dimensional sphere. This simple parsimonious model requires only a few assumptions, excluding dark energy to satisfy the Cosmological Constant Λ, and is shown to match the Universal expansion rate, as established from supernova cosmology survey points. This novel model conceives the universe as a higher dimensional dynamic with spacetime as a projection, rather than as an arrow from absolute beginning of the big bang. Red-shifting is alternatively proposed as azimuthal angular projections of wavelengths λ. Accelerated Universal Expansion is alternatively proposed as azimuthal projections of meridians, asymptotical to a horizon, and Lambert's cosine law of luminous intensity.
A radical implication of this model is that azimuthal angular projections are positional dependent, and thus it's conceivable that apparent distances between galaxies vary with the location of the observer (see figure 4). Supportive mathematical evidence is described from the Hubble Tension; Discrepancies between visible spectra red-shifting of cepheid variables (the most recent calculation is $Ho = 74.03 \pm 1.42 km/sec/Mpc$), and from temperature fluctuations in the Cosmic Microwave Background (CMB) (which are calculated to be $Ho = 68.7 \pm 1.3 km/sec/Mpc$), which resolves the discrepancy by recalibrating redshift data from supernova Cosmology survey points.

Keywords dark matter · Hubble tension · galaxy rotation curve · accelerated universal expansion

1 Introduction

This novel conceptual model upends the cosmological timeline, red-shifting, and accelerating universal expansion. This article begins by describing how global meridians, which are azimuthally projected onto a flat surface, are asymptotic along the surface, toward the horizon (away from the observer), in the familiar "Atlas" (gnomonic projected) mapping. By extension, the hyper-meridians of a $\mathbb{R}^4$ (four spatial) dimensional hypershere, azimuthally projected onto a $\mathbb{R}^3$ (three spatial) dimensional sphere, are shown to be asymptotic along the spherical surface and also away from the observer. A coordinate system is presented (in a cross section) to equate red-shifting of wavelengths λ with azimuthal angular projections, Using this equation, red-shift (z) is revised from: $z = \frac{\lambda_{obs} - \lambda_{rest}}{\lambda_{rest}}$ to be a function of distance x_n and hyperspere arc length (radian) $z = \frac{\lambda \frac{x_n}{a} - \lambda}{\lambda}$. In conjunction with observed red-shifting survey data and Lambert's cosine law of luminous intensity, the universal hyperspere radius is estimated. From these established parameters, it is shown how both velocity and energy density appear to increase along azimuthally projected (skewed) length (x). As well, how galaxies appear to be dilated (or elongated), along the line of sight, with a resulting flattened rotation curve. From these established parameters, a function is developed to plot a curve, which is superimposed upon graphs (Distance modulus (μ) vs red-shift (z)) of data points from the HST Key Project. discrepancies between theoretical and observed galaxy rotation curves, as well as apparent increased energy density are shown to be predicted from this model.

2 Intuition of the Azimulthal Hyper-Projection Model of Cosmology

The familiar Atlas map, which is an $\mathbb{R}^2$ azimuthal global projection, typically places Siberia and Alaska at opposite extremes. However, they are locally connected at the Bering Strait, as viewed in $\mathbb{R}^3$ space. See figure 1.

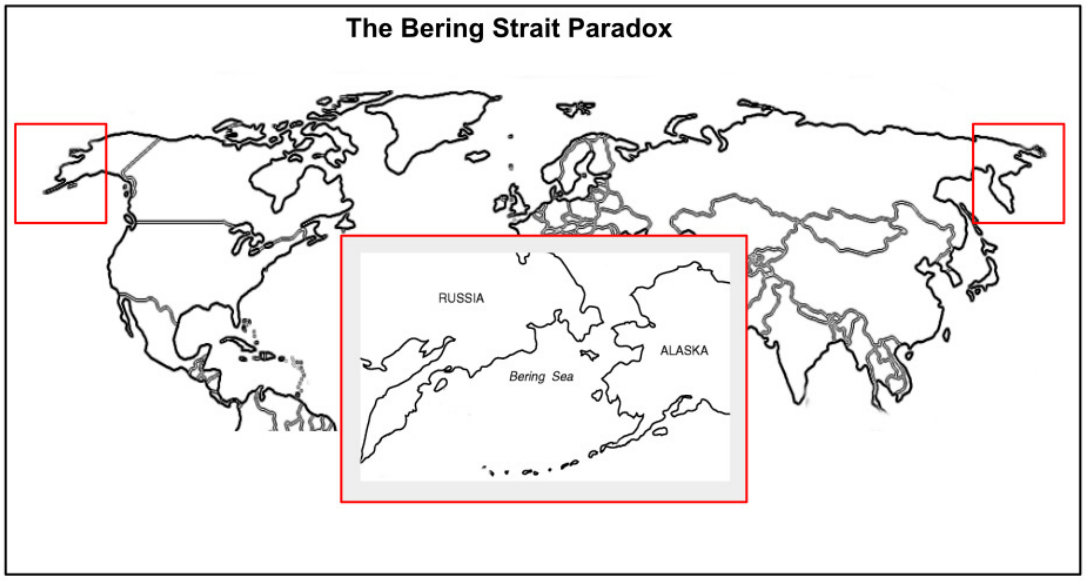

Figure 1: Atlas map, which is an $\mathbb{R}^2$ azimuthal global projection

The Azimulthal Hyper-Projection Model of Cosmology proposes the following hypothesis:

Hypothesis 1 (H1) *As an Azimulthal Hyper-Projection onto spacetime is asymptotic to an outward horizon, the geometric perspective is based to the position of the observer, such that all projected geodesics will appear to be expanded outwardly, from the arbitrary biased perspective of the observer. This effect is similar to the familiar atlas map, which when viewed from North America, typically places Siberia and Alaska at opposite extremes. Therefore, the apparent distances between remote galaxies could actually be local neighbors, and vice versa, from their perspective.*

Azimuthal Projections onto an $\mathbb{R}^2$ Plane Appear to Expand Outward from the Observer, along the plane

Figure 2 shows an observer on a $\mathbb{R}^2$ plane, positioned along a tangent of a $\mathbb{R}^3$ sphere, measures projected meridians at distance x_n, per the equation [1]:

$$x_n = R\ tan(\theta) \tag{1}$$

Figure 3 shows how azimuthally projected meridians are asymptotic along the $\mathbb{R}^2$ plane, and toward the horizon (away from the observer).

Figure 4 shows how azimuthal projections expansion is relative to the observer's position. On the left side, the observer is positioned along a tangent at projection a, and expansion increases toward point g. However on the right side, the observer is positioned along a tangent at projection g, and expansion increases toward point a.

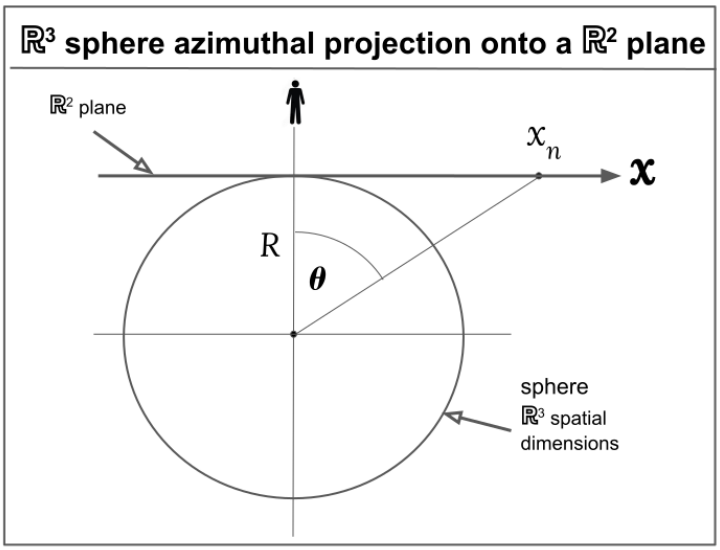

Figure 2: $\mathbb{R}^3$ sphere azimuthally projected onto a $\mathbb{R}^2$ plane. Distance from angle θ and radius of sphere.

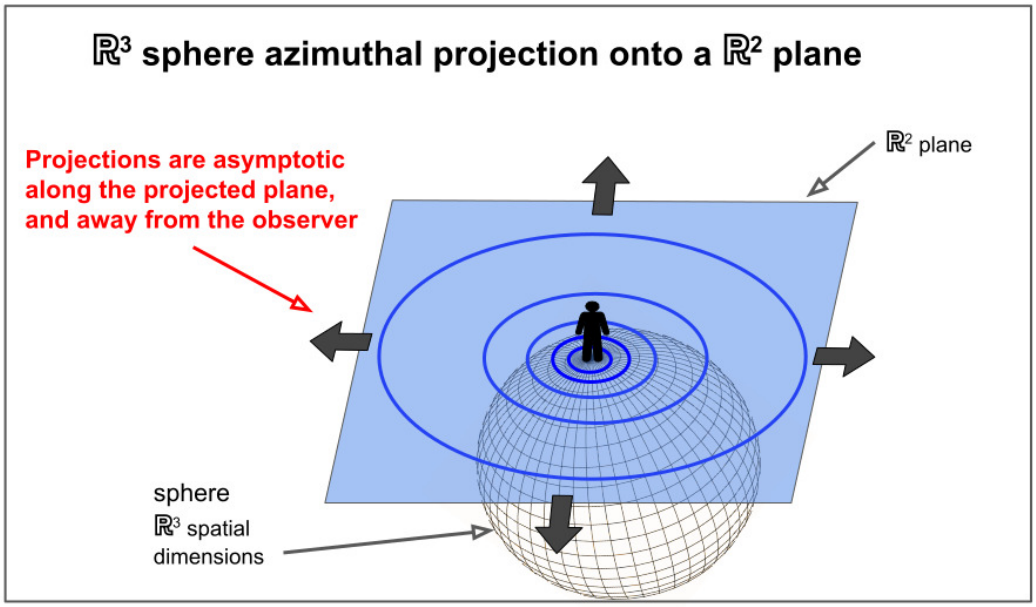

Figure 3: meridians are asymptotic along the $\mathbb{R}^2$ plane, and toward the horizon (away from the observer).

Positional Dependence of Projection Expansion

3 $\mathbb{R}^4$ Hypersphere Azimuthal Projections onto an $\mathbb{R}^3$ Sphere Appear to Expand outward from the Observer in three spacial dimensions

Figure 5 shows how azimuthally projected hyper-meridians are asymptotic along the $\mathbb{R}^3$ sphere, and outward from the observer.

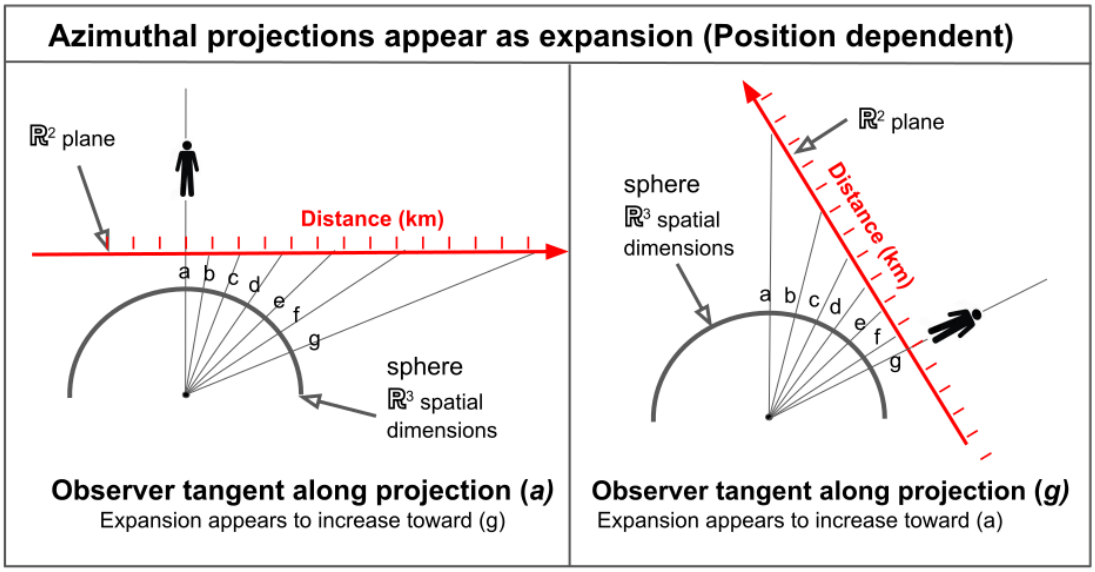

Figure 4: Azimuthal projections appear as expansion (Position dependent)

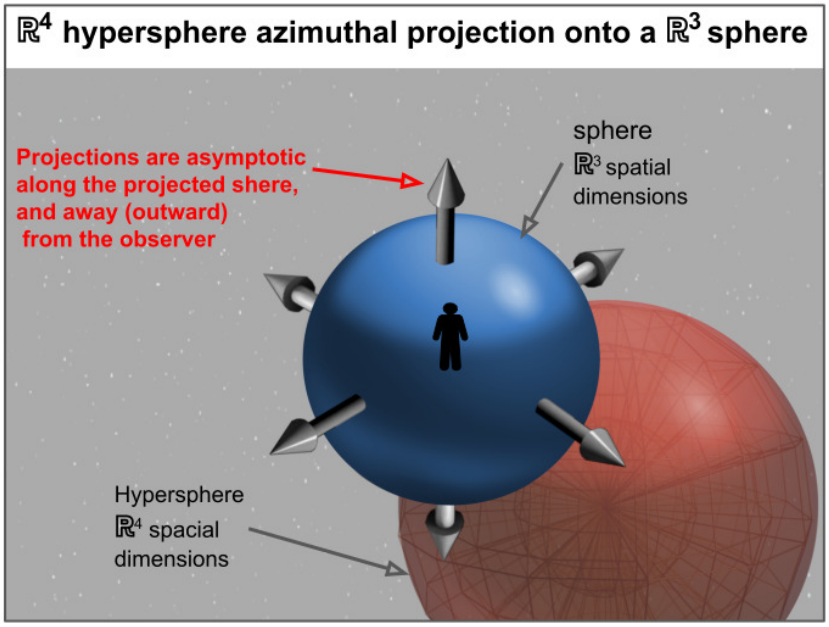

Figure 5: $\mathbb{R}^4$ hypersphere azimuthally projected onto a $\mathbb{R}^3$ sphere. hyper-meridians are projected asymptotic along the sphere, and away from the observer.

Figures 6 and 7 show how azimuthal projections red-shifting is relative to the observer's position. On the left side, the observer is positioned along a tangent at projection *a*, and red-shifting increases toward point *g*. However on the right side, the observer is positioned along a tangent at projection *g*, and red-shifting increases toward point *a*. A radical implication of this model is that azimuthal angular projections are positional dependent, thus degrees of redshifting over distance is positional dependent. It's conceivable that our local group would appear to be much more expanded, from the perspective of remote observer, and vice versa; vastly remote galaxies would appear to spaced much closer together, from the perspective of a remote observer.

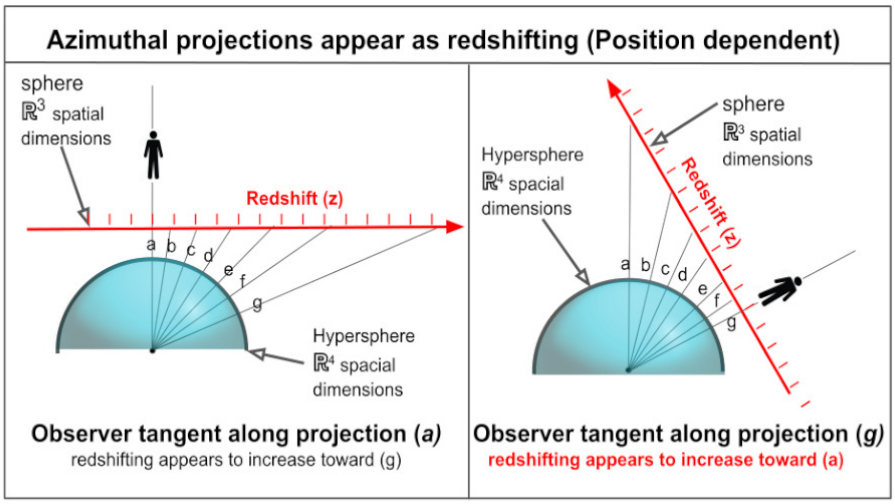

Figure 6: Azimuthal projections appear as red-shifting (Position dependent)

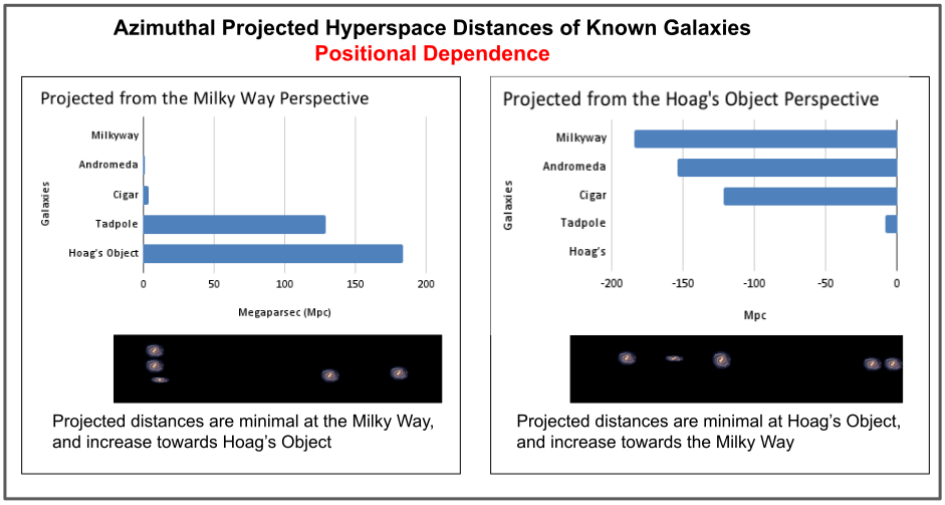

Figure 7: Positional Dependence of known Galaxies

4 Red-shifting is Alternatively Proposed as Azimuthal Angular Projections of Wavelengths λ

As Azimuthal projections are asymptotic along the observer's line of sight, obliqueness increases with distance x. Thus wave lengths become stretched along the observer's line of sight x. The observer in spacetime can not directly observe the projections in hyperspace, and is limited to his line of sight on the x direction. Figure 8 shows how the observer measures the wave lengths λ to be skewed (red-shifted). Section $B-B$, the "at rest" wavelength λ_{rest}, is normal to the hypersheric surface. Oblique view $A-A$ is the "observed" wavelength λ_{obs}, with a skewed (elongated) wavelength.

5 Revised Formula for Red-shiff (z)

Figure 9 is a 2 dimensional cross section of an $\mathbb{R}^4$ (spatial dimensions) hypersphere Azimuthal projected onto a $\mathbb{R}^3$ (spatial dimensions) sphere, and extended along X axis into macrospace. A classic space observer resides along the X axis at reference frame: $x=0$, from which all measurements ($x_n \neq 0$) are skewed projections, asymptotic to the horizon.

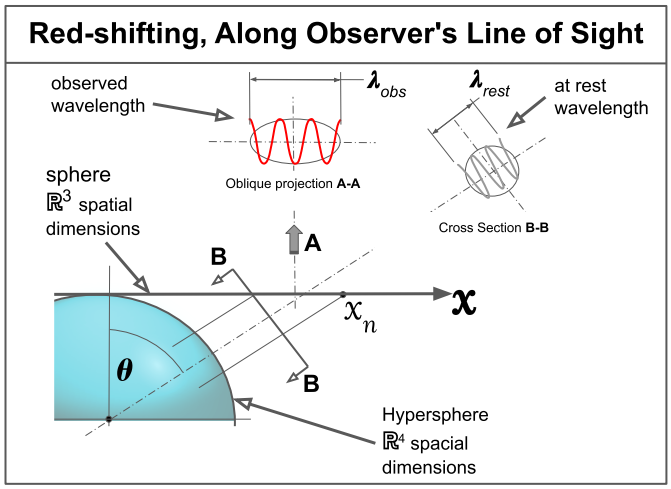

Figure 8: Red-shifting, Along Observer's Line of Sight.

$$S \in \mathbb{R}^2 def = (x, y) || \sqrt{x^2 + y^2} = r || \tag{2}$$

$$F : S \rightarrow I(x) \left[0, x_n\right] \tag{3}$$

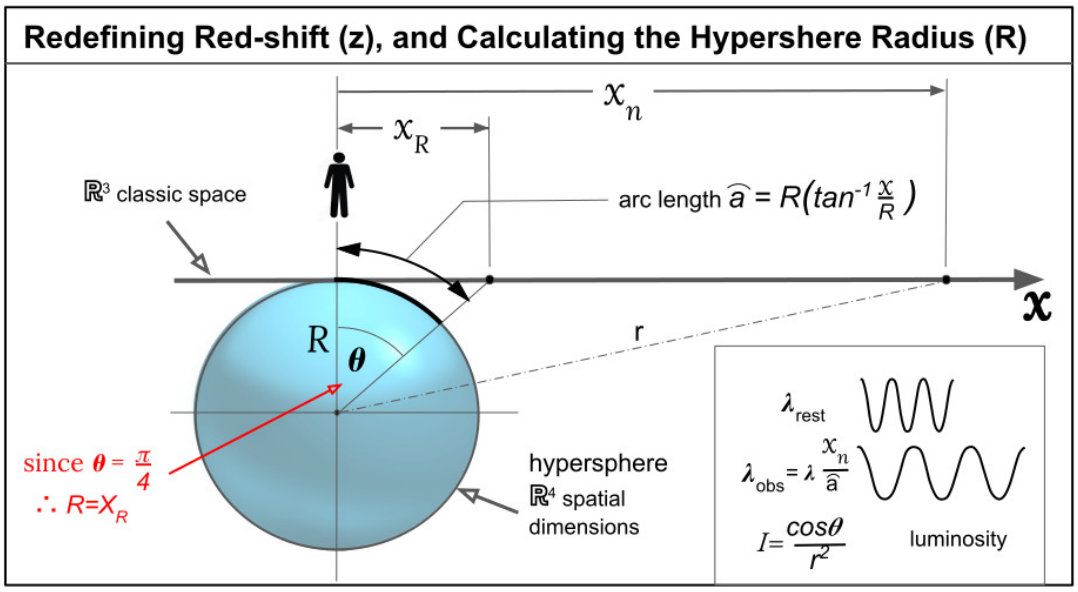

Figure 9: Revised redshift (z), and radius of hypershere

Hyper-meridians and celestial bodies are Azimuthally projected as lateral straight lines, per equation 5:

$$x_n = R \, tan \, \theta$$

Solving for R:

$$R = \frac{x_n}{tan \, \theta} \tag{4}$$

$$\widehat{a} = R\,\theta \implies \tag{5}$$

$$\widehat{a} = R\left(\arctan\frac{x}{R}\right) \tag{6}$$

Framed within this model, electromagnetic wavelengths of λ, along the hypersphere circumference of radius R, are considered to be at rest. However, x_n is projected (skewed) along the X axis and observed with resulting redshift (z), similar to the redshifting equation [2]:

$$z = \frac{\lambda_{obs} - \lambda_{rest}}{\lambda_{rest}} \tag{7}$$

In this alternative model, $\lambda_{obs} = \lambda\frac{x_n}{\widehat{a}}$,

$$z = \frac{\lambda\frac{x_n}{\widehat{a}} - \lambda}{\lambda} \tag{8}$$

Calculating the Universal Hypersphere Radius

The radius R of the hypershere can be deduced from a spacetime perspective (Where humans reside), by considering, that observed **distance (x_R) must be equal to radius R when the tan of θ is equal to 1, or when $\theta = \frac{\pi}{4}$**. Thus from the z value, where $\widehat{a} = R\frac{\pi}{4}$, and $x_R = R$, radius R is derived,

$$\widehat{a} = R\left(\frac{\pi}{4}\right) \qquad Substituting\ \frac{\pi}{4}\ for\ \theta\ in\ equation\ 5 \tag{9}$$

$$z = \frac{\lambda\left(\frac{x_n}{R\frac{\pi}{4}}\right) - \lambda}{\lambda} \qquad Inserting\ into\ equation\ 8 \tag{10}$$

$$z = \frac{x_n}{R\left(\frac{\pi}{4}\right)} - 1 \qquad cancelling\ \lambda \tag{11}$$

$$z = \frac{R}{R\left(\frac{\pi}{4}\right)} - 1 \qquad Since\ x_n = R, \tag{12}$$

$$z = \left(\frac{4}{\pi}\right) - 1 \qquad Simplifies\ to, \tag{13}$$

$$z = 0.273 \tag{14}$$

Finding R from $z = 0.273$, using the approximate distance formula,

$$d \approx \frac{zc}{H_0} \tag{15}$$

At current H_0 value of: $73.8 km/sec/Mpc$

$$R \approx \frac{0.273 * 299792 km/sec}{73.8 km/sec/Mpc} \implies \tag{16}$$

Thus, the radius of the $\mathbb{R}^5$ hypersphere,

$$R \approx 1108.987\ Mpc \tag{17}$$

6 Accelerated Universal Expansion is Alternatively Proposed, as $\mathbb{R}^5$ Azimuthal Projections of Meridians, Asymptotical to a Horizon, and Lambert's Cosine law of Luminous Intensity

Velocity Appears to Increase Along Projected Length x_n

In figure 9. Light-waves and energy density are constant along arc length $\widehat{a}$. However,

Theorem 1 *As $\mathbb{R}^5$ hyper-spacetime is azimuthal projected onto $\mathbb{R}^4$ spacetime, From the r.f. of an observer on the projected surface, topology is skewed (elongated), and appears expanded outward from the observer. As a result, celestial bodies appear to be traveling along expanded projected geodesics with increasing velocities (v). This apparent increase of velocity is equivalent to a decreased time interval ($-\Delta t$). Light-waves appear to travel along X_n with an increased velocity $\vec{v}'$ of:*

$$\frac{\vec{v}'}{\vec{v}} = \frac{X_n}{\widehat{a}} \tag{18}$$

Calculating z per Distance x

Now that R (The radius of the hypersphere) has been established, values of z can be determined from any value of x_n. Note that x_n is a one dimensional cross-section of the space which humans measure galactic distance, although it is actually a skewed projection of hyper-arc length $\widehat{a}$ onto classic space. Thus, from values of distance modulus μ and established radius R, theta is easily determined. Subsequently from theta, $\widehat{a}$ is determined. Finally from equation 8, z is derived at any distance x_n.

Energy Density Increases along Length X_n

Corollary 1.1 *As velocity along skewed x appears to increase per equation 18, energy density ρ proportionally increases, due to increased velocities in particle kinetic and internal energies (compression, energy of nuclear binding, etc.). The observer at $x = 0$ measures volume at x_n [mpc] with increased energy density ρ_n per equation:*

$$\frac{\Delta\rho_n}{\Delta\rho} = \frac{(x_n - R)}{R}$$

Lambert's Cosine Law of Illumination

Consider that figure 9 describes an oblique projection of a source S with an illuminate value I. According to Lambert's Cosine Law of illumination [3], intrinsic values of such projected light will decrease in value with θ per equation:

$$I = \frac{\cos\theta}{r^2} \tag{19}$$

In this model, the luminous intensity of type Ia supernovae would decrease, accordingly. Thus, conventionally accepted standard candle measurements along x, would need to be recalculated per Lambert's Cosine Law.

7 Galaxy Rotation Curve with Increased Density

The discrepancies between theoretical and observed galaxy rotation curves involve both density and velocity. Conventionally, the dependence of circular velocity V_{circ} on radial distance R assumes M, m and velocity to be fixed over large scales in Kepler's law, [4]

$$T^2 = \frac{4\pi^2 r^3}{GM} \Rightarrow T^2 \propto r^3$$

Moreover, gravitational lensing demonstrates the existence of a much greater Mass (density) than the sum of the stars within the galaxy. **However, this alternate model specifically addresses these two issues and provides an alternative explanation,**

Kepler's Law rearranged as density ρ integrated over time dt

Corollary 1.2 *Velocity $\vec{v}$ and density ρ_n are measured with increased magnitude per distance x_n. This directly extends to energy density within galaxies and the effects on rotational velocity, such that: As x_n increases, centripetal force is perfectly balanced by increases in $\vec{v}$ and, subsequently, ρ_n,*

$$\frac{v^2}{r} = \frac{G}{r^2}M = \frac{G}{r^2}\int \rho_n dt$$

Note: total mass M inside the circle of the radius r can be obtained by doing integration of mass density in a volume. $M = \int \rho_n dt$. $\rho = \rho_R$ and ρ_M (Dark components are excluded from this model, with the intent of presenting an alternative).
Figure 11 shows how skewed projected meridians, along the observer's line of sight, appear elongated and are measured with greater density. The result is a flattened rotation curve, per $\frac{x}{\widehat{a}}$. Thus, an elongated galaxy appears to have greater rotational velocity, and energy density.

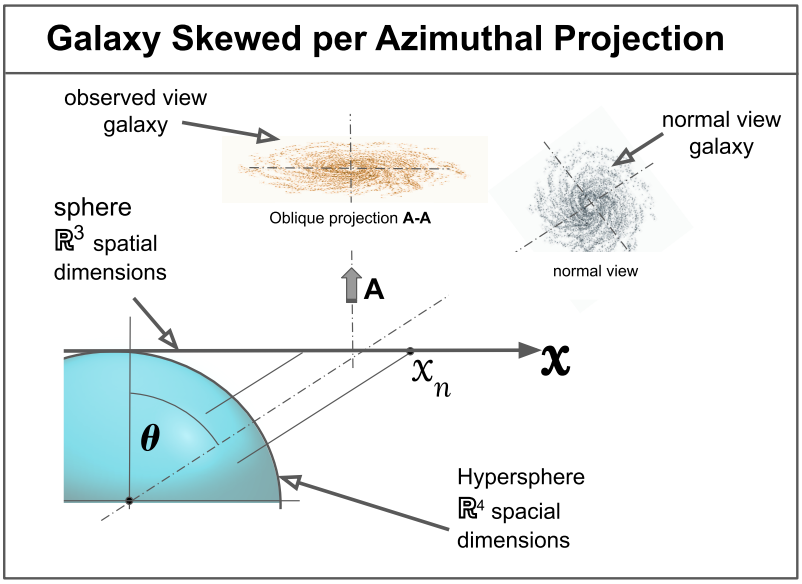

Figure 10: Spiral galaxy projection is skewed

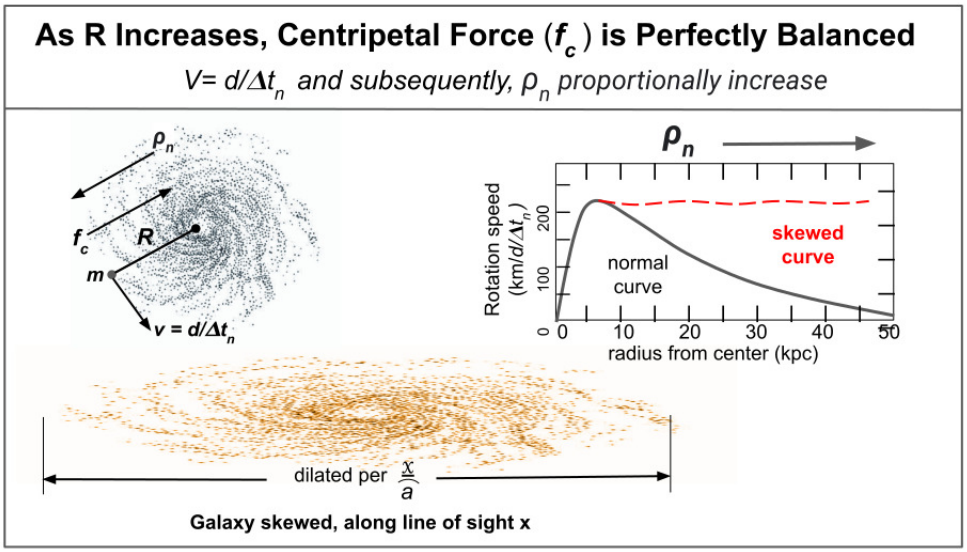

Figure 11: Elongated galaxy appears to have greater rotational velocity, and energy density.

$$\lim_{r\to -r_n} \frac{\partial \rho}{\partial (ar)} = \lim_{r\to +r_n} \frac{\partial \rho_n}{\partial (ar)}$$

8 Graphing a Function that conforms with the Hubble Diagram

From this model of higher dimensional gnomonic projection, function $F(z)$ provides a graph to compare with Supernova Cosmology Survey Points. Using z as the dependent variable, and μ as independent variable, such that $F(z)$ is a function of μ. From x_n in equation 7, Using equation 6, and converting R to mega parsecs.

$$\lambda X_n = \left(\lambda_{rest} \frac{x}{1108.987\left(\arctan \frac{x}{1108.987}\right)}\right) \tag{20}$$

Inserting into equation 7,

$$z = \left[\frac{\left(\lambda_{rest} \frac{x}{1108.987\left(\arctan \frac{x}{1108.987} \right)} \right) - \lambda_{rest}}{\lambda_{rest}} \right] \tag{21}$$

λ_{rest} cancels, leaving,

$$z = \left[\left(\frac{x}{1108.987\left(\arctan \frac{x}{1108.987} \right)} \right) \right] - 1 \tag{22}$$

Converting redshift z to velocity km/sec,

$$F = \left[\left(\frac{x}{1108.987\left(\arctan \frac{x}{1108.987} \right)} \right) - 1 \right] * 300,000 km/sec \tag{23}$$

Substituting Lambert's equation (19) for x,

$$F = \left| \left(\frac{x(1108.987 * cos((\arctan(\frac{x}{1108.987}))))}{\left(\frac{cos\left(\left(\arctan\left(\frac{x}{1108.987} \right) \right)}{x^2 + 1108.987^2} \right) \right)^2 + 1108.987^2} \right) - 1 \right| * cK \tag{24}$$

Where K is a slope correction constant, which is necessary to offset conventional measurements of standard candle distances.

Table 1 lists extrapolated points, at $50(Mpc)$ intervals, of Function $F : d \mapsto v \mid F = \{v, f(d)\}[0.000, 5x10^8]$. Also, corresponding values of μ and z

Figure 12 shows the Function $F : d \mapsto v \mid F = \{v, f(d)\}[0.000, 5x10^8]$

Table 1: Extrapolated points of function F. In successive columns:, [pc] (distance parsec), [km/s] (kilometers per second), [μ] (Distance modulus), [z] (redshift),

pc	**km/s**	μ	**z**
5.000E+07	4.129E+03	33.495	0.014
1.000E+08	8.228E+03	35.000	0.027
1.500E+08	1.227E+04	35.880	0.041
2.000E+08	1.622E+04	36.505	0.054
2.500E+08	2.006E+04	36.990	0.067
3.000E+08	2.377E+04	37.386	0.079
3.500E+08	2.734E+04	37.720	0.091
4.000E+08	3.074E+04	38.010	0.103
4.500E+08	3.397E+04	38.266	0.113
5.000E+08	3.703E+04	38.495	0.124

Figure 13 shows the Function $F : z \mapsto \mu \mid F = \{\mu, f(z)\}[0.000, 0.125]$. **Note the familiar curve (in logarithmic scale), which is conventionally interpreted as "accelerated expansion"**.

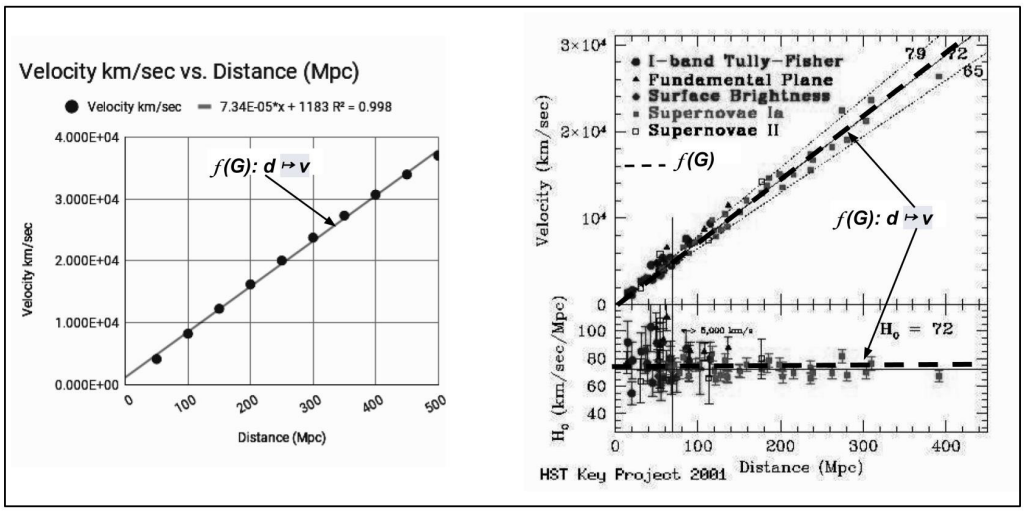

Figure 12: Left: Function $F : d \mapsto v$, with extrapolated points. Right: Function F superimposed onto the HST Key Project

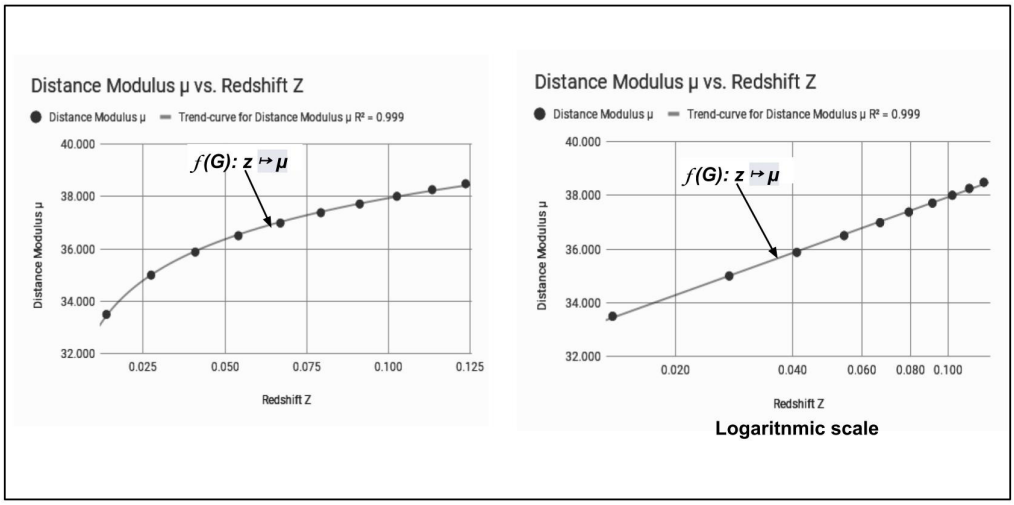

Figure 13: Left: Function $F : z \mapsto \mu$, with extrapolated points. Right: Function F with logarithmic scale, along z axis. **Note the familiar curve, which is conventionally interpreted as "accelerated expansion".**

9 Supportive Evidence of the $\mathbb{R}^5$ Azimuthal Projection Model

Galaxy Recession velocities (z red-shift and blue-shift) will be measured greater on the far side of galaxies. Such a closed system expanding in azimuthal projected hyperspace **would defy the standard model of accelerated universal expansion and dark energy**, where only space between galaxies are assumed to be expanding. Theorem 1, is supported by the following correlation study[5] "On Possible Systematic Redshifts Across the Disks of Galaxies" . This study shows a deviation from Kepler's orbital laws, specifically on the subject of increased velocity on the far sides of multiple galaxies. Although not conclusive, it does justify consideration to this article.

Note that multiple galaxy surveys with increased velocities across their minor axis. Thus, **velocity within the same body appears to increase per distance.** "Velocity observations in 25 galaxies have been examined for possible systematic redshifts across their disks: a possible origin for the redshifts could be the radiation fields. Velocities increase towards the far sides in most cases. This is so for the ionized gas, for neutral hydrogen, and in some cases for the stars. The effect is seen as velocity gradients along the minor axes, as well as in velocity fields of neutral hydrogen in other parts of the galaxies. Deviation of the kinematic major axis from the optical axis is found for 10 galaxies and in 9 of these the largest velocities occur in the far side. In the central regions of four galaxies are found large velocity gradients in the same direction. While expanding motions provide an explanation for some of these features, it remains difficult to thereby explain all the peculiarities found. Faintness of the data available in this preliminary study should be noticed. Observations specially programmed for this subject would be necessary."

table 2 lists 25 galaxies, correlation coefficients and relevant columns (including sources of data):

Table 2: List of galaxies for which velocities along the minor axies are available. In successive columns: type; distance; angle between rotation axis of galaxy and line of sight; regression and correlation coefficients between velocity and distance; source of data

NGC	Type	d(Mpc)	i	$h(kms^{-1}kpc^{-1})$	corr	source of data
244	Sb	0.69	77°	0.20	0.272	Gottsman and Davis (1970)
253	Sc	4.0	78	0.13	0.012	Burbridge et al. (1963a)
300	Sd	2.4	43	1.03	0.844	Shobbrook and Robinson (1967)
598	Scd	0.72	57	1.51	0.866	Goordon (1971)
613	SBbc	15	47	57.09	0.820	Burbridge et al. (1964c)
972	SBc	17	66	-11.31	-0.670	Burbridge et al. (1964c)
1084	Sc	14	65	-4.75	-0.338	Burbridge et al. (1965)
1097	SBd	12	50	5.00	-0.105	Burbridge and Burbridge (1960)
1365	SBd	15	66	-79.21	-0.976	Burbridge et al. (1962a)
1792	Sbc	10	64	10.12	-0.578	Rubin et al. (1964)
2403	Scd	3.3	55	0.04	0.118	Burns and Morton (1971)
3310	Sbc	11	31	61.27	0.815	Walker and Chincarini (1967)
3521	Sbc	7.6	66	7.18	0.056	Burbridge et al. (1964b)
4736	Sab	3.3	40	44.28	0.849	Walker and Chincarini (1967)
4826	Sab	7.3	60	39.16	0.854	Rubin et al. (1965)
5194	Sbc	4.0	35	-15.18	-0.758	Burbridge et al. (1964a)
5248	Sbc	11	55	-26.94	-0.690	Burbridge et al. (1962b)
5457	Scd	3.5	27	-1.40	-0.403	Rogstad and Stoshak (1971)
6574	Sba	33	45	4.73	0.428	Demoulin and Tung Chan (1969)
27469	Sa	51	49	8.69	0.552	Burbridge et al. (1963c)

10 Observational Phenomena of the $\mathbb{R}^5$ Azimuthal Projection Model

The Azimuthal Projection Model implies two observational phenomena for research and experimentation:

- The planets in our solar system will deviate from their Kepler / Newtonian orbits by an increased radius and velocity, as their distance from Earth increases. Figure 14 is exaggerated for clarity.
- Two opposing zenith vantage points in the solar system (Earth vs the most outer region), in azimuthal projected hyperspace, will measure planetary distances as opposing skewed geometry, such that (respectively) projected distances are locally and remotely maximized. Figure 15 is exaggerated for clarity.

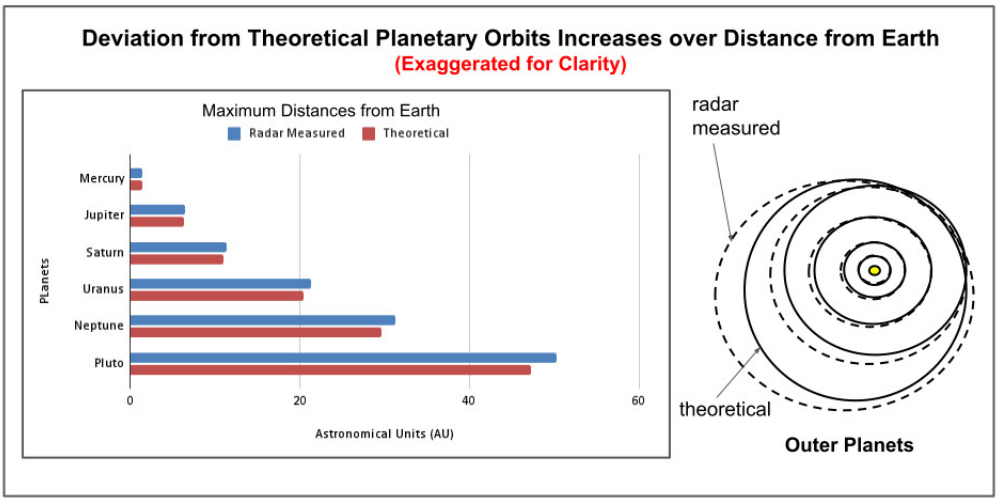

Figure 14: Deviation from Theoretical Planetary Orbits Increases over Distance from Earth

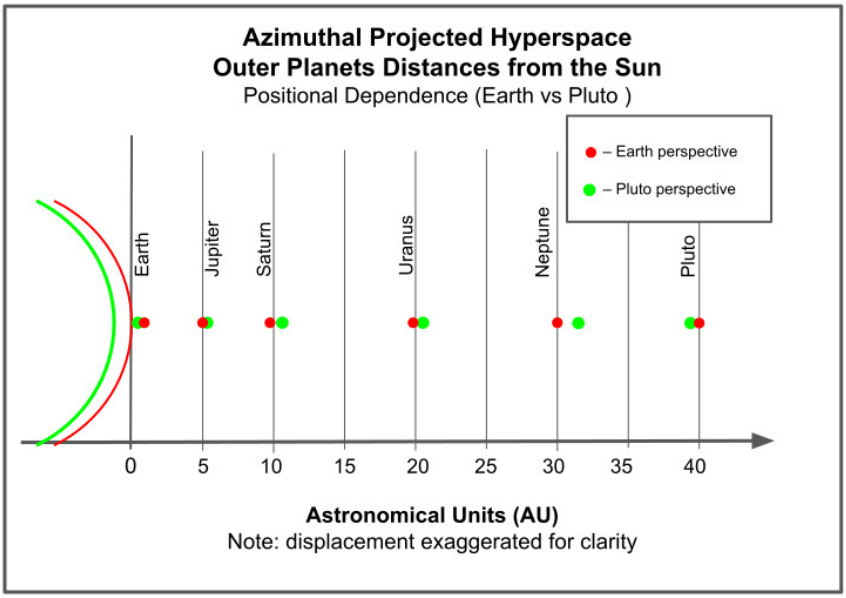

Figure 15: Two opposing projections of planetary distances

11 Why then do the Most Distant Galaxies Appear Fully Developed?

The James Webb Space Telescope (JWST) observations of the most distant galaxies, some formed just 330 million years after the Big Bang when the universe was a mere 2 percent of its current age, appear as no less developed than our local group. **Consequently, such observations compel theorists to rethink current standard models**. Just as The Azimuthal Projection Model of Universal Expansion implies that our Milky Way galaxy's rotational curve would appear greatly accelerated and flattened from vast distances, it predicts the JWST observations as well. The fundamental concept of this model, is that redshifting is viewer dependent, and a function of projection at any given point. Thus, the radical implication is that the universe must be conceived of as a higher dimensional dynamic with spacetime as a limited projection which is viewer dependent, rather than as an arrow from absolute beginning of the big bang.

12 Conclusion

This parsimonious model, is based solely on a few assumptions. it does not require dark energy to satisfy the Cosmological Constant Λ. It implies a smaller universe than conventional estimates, and the universal hypersphere radius is easily derived. A great many mysteries are resolved, including galaxy rotation curves, accelerated expansion, as well as increased energy density. In summary, it is conceptually more reasonable.

Data Availability Statement: No Data associated in the manuscript

References

[1] Coxeter H. Introduction to Geometry (2). Wiley, Manhattan, 1969.

[2] Taylor E and Wheeler JA. Spacetime Physics. WH Freeman and Company, New York, 1992.

[3] R Waynant. Electro-Optics Handbook. McGraw-Hill, 1994.

[4] Butikov E. Motions of Celestial Bodies. IOP Publishing, Philadelphia, 2014.

[5] T. Jaakkola, P. Teerikorpi, and K. Donner. On possible systematic redshift across the disks of galaxies. Astronomy and Astrophysics., 1975.